AERODYNAMIC PARAMETRIC STUDY OF HELICOPTER ENGINE NOZZLE

Thaenan dos Reis Marioni, Laurent Sudre
Eurocopter (France)
e-mail: thaenan.dos-reis-marioni@eurocopter.com
e-mail: laurent.sudre@eurocopter.com

Abstract

This paper presents a Computational Fluid Dynamics (CFD) analysis on the influence of different geometric parameters and aerodynamic conditions on the performance of a helicopter exhaust nozzle system, namely the pumping ratio and the recovery pressure. Through automatic 2D axisymmetric and 3D CFD simulations of a simplified but representative exhaust system of variable geometry, the aim of this work was to identify and relate the behavior of the flow to a physical design parameter whenever possible. It was shown that while some parameters may have small impact on the performance, e.g. ejector inlet lip radius, others such as the ejector diameter and length and nozzle diffusion are essential to an optimization process. Also, results have shown that changes in the geometry systematically leads to conflicting results in terms of ventilation and power loss, forcing the design to be based on a trade-off between these quantities. Moreover, it was observed that ejector elbow angle and inlet swirl are strongly coupled. Finally, in this paper it is pointed out that the shape of the primary nozzle and the decentering of ejector and primary nozzle axes are two design parameters that can help improving the pumping ratio without important degradation of the recovery pressure.

1. NOMENCLATURE

α	Distance from input parameters space center
C_p	Pressure recovery coefficient
CCD	Central Composite Design
ΔP	Total pressure drop
D_E	Ejector inlet diameter
D_N	Nozzle exit diameter
DOE	Design of Experiments
ϕ	Pumping ratio
f	Fraction of factorial design
L	Ejector overall length
$\dot{m}$	Mass flow rate
M	Mach number
MTOP	Maximum Take-Off Power
N	Number of parameters
OAT	Outside Air Temperature
$\bar{p}_s$	Area-weighted average of static pressure
$\hat{p}_{dyn}$	Mass-weighted average of dynamic pressure
r	Spearman correlation coefficient
σ_{xy}	Covariance
s	Standoff
y^+	Normalized wall distance

2. INTRODUCTION

In general, an exhaust duct is placed at the engine exit in order to recover some of the static pressure of the jet by decelerating the flow. On a helicopter, the engine exhaust system can also be used to fulfill other functions, such as:

- orienting the ejection of engine hot gases to avoid reingestion and tail boom heating
- ventilating the engine compartment to ensure correct temperature conditions for the installed equipment
- improving engine hot gases and fresh air mixing for infrared signature reduction

This can be accomplished by placing downstream of the engine nozzle a second nozzle of larger diameter (called ejector). Due to the pressure difference at the space between these two elements and to viscosity effects, a flow is created inside the engine compartment (Venturi effect, Figure 1).

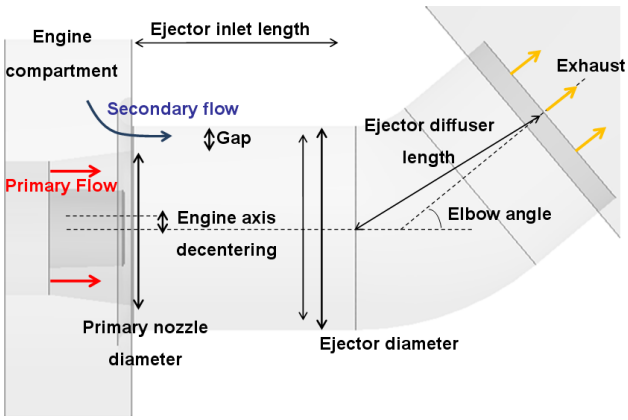

Figure 1 Venturi effect scheme and some of the geometric parameters considered in this study

Many constraints are to be considered in the design process of such exhaust systems:

- Safety: the correct ventilation and the safety of the aircraft in case of fire in the engine compartment must be ensured at all times.
- Installation: the available cowling volume limits the dimension of the ejector, sometimes even imposes a determined length.
- Engine performance: minimize installation power losses.

The efficiency of the air suction into the engine compartment is measured by the pumping ratio ϕ, which is defined as the ratio between entrained and primary flows. When normalized by the square root of primary and secondary temperatures ratio, this quantity does not depend on the temperature[1] and thus on the engine rating. It is found in the literature[2] that some of the most impacting geometric parameters on the performance of an ejector are its length, the entrance area compared to primary nozzle exit area (area ratio) and the axial distance between primary nozzle and ejector.

Clearly, the presence of the ejector and the secondary airflow induction make the pressure drop of the exhaust system increase compared to an isolated test bench primary nozzle and, as a consequence, the engine power losses are higher. Moreover, pressure recovery and pumping ratio are often conflicting quantities resulting in a trade-off between these parameters in the design process.

Many studies have been performed on diffuser and ejector design and several methods proposing a global evaluation of a configuration were developed. For example, one-dimensional approaches[3], with or without swirl effect corrections[4], can provide a first approximation of the pumping ratio. For the recovery pressure, Sovran & Klomp's iso-C_p curves[5] give a fair estimation of the superior limit of the recovery pressure as a function of aspect ratio and normalized length of diffusers. However, understanding how these geometric parameters affect the flow and the performances is not obvious. How strongly they are correlated is also of interest.

This paper presents a CFD analysis on the influence of some geometric parameters (some of which are represented in Figure 1) and aerodynamic conditions on the performance of the exhaust system, measured by the pumping ratio and recovery pressure, always taking into account safety constraints and system size. Through fully automated 2D axisymmetric and 3D CFD simulations of a simplified but representative exhaust system of variable geometry and a design exploration based on response surfaces, the aim of this work was to identify and relate the behavior of the flow to a physical design parameter whenever possible.

3. MODELLING AND PARAMETERIZATION

3.1. Geometry and mesh

A fully automated CFD simulation process was set up using Ansys Workbench®, which integrates all steps of a CFD study, namely geometry design, mesh generation, computation and post-processing, and provides the user with the possibility of defining input and output parameters which can then be used for design exploration and optimization.

For both the axisymmetric 2D and the 3D analysis a simplified model of a helicopter exhaust system was created. The computation domain consisted of a primary nozzle and its central body and an ejector placed downstream and of larger diameter so there is a gap between these two elements. The struts which usually hold the nozzle to the central body were not simulated in this study. The initial dimensions and positions were based on existing designs to ensure the results to be representative.

The engine compartment was modeled by a fluid domain placed upstream of the ejector and at its exit a sufficiently large dump domain was added to correctly simulate the mixing within the ejector and the exhaust into the atmosphere (Figure 2).

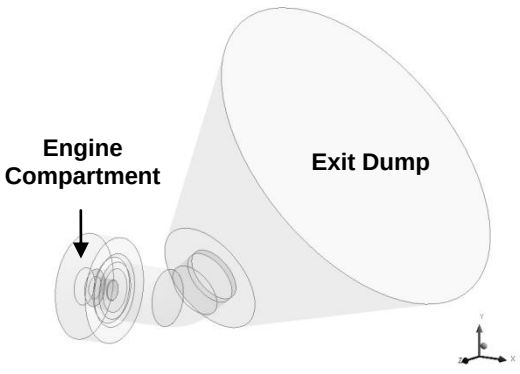

Figure 2 3D computational domain

The unstructured mesh generation process was automated using Ansys Meshing®. Three prisms layers were added near to the wall to account for the boundary layer and in the most significant zones of the flow, i.e. the gap, the mixing region and the exhaust jet, a refinement of the mesh was imposed. The parameterization of the refinement functions

allowed the reproducibility of the mesh characteristics for all tested configurations.

Typically, the mesh was composed of 20000 elements in 2D analysis and 5 million elements in 3D analysis. A mesh size study was performed to determine the best compromise between solution independence and computational time and it was shown that beyond the retained refinement, the variations of the solution are smaller than 1% while the computational time increases by 50%. It was also verified that the upstream domain and the exit dump are sufficiently large not to affect the solution.

The simulations were performed using Ansys Fluent® 14.0, which uses a finite volume method to solve the Navier-Stokes equations. The air is defined as an ideal-gas and the viscosity varies with the temperature according to the Sutherland Law. The spatial discretization schemes of all quantities except the pressure were set to the second order and the least squares cell-based option was chosen. A coupled solver with pseudo-transient option was employed with an aggressive length scale method definition. The convergence criterion was based not only on the residuals but also on physical quantities such as mass flow rate and total pressure mean value at the ejector exit: once the variations are smaller than a user-defined tolerance, the solution is considered as converged and the iterations are automatically stopped.

Studies on the ability of CFD models to predict the flow of diffusers and ejectors compared to experimental results[6] have demonstrated that most of the commonly used turbulence models reasonably represent the global features of the flow, but the performance prediction strongly varies from one to another. It was shown[7] that SST $k-\omega$ turbulence model is well adapted for high-shear and swirl flows and can provide fair estimations of pumping ratio and pressure recovery. This model was chosen for the present study and to correctly account for boundary layer effects, the mesh was generated to ensure $y^+ \approx 1$ on the primary nozzle and ejector walls and $y^+ < 5$ elsewhere.

Since engine compartment ventilation leads to pressure losses and airflow heating, a negative total pressure was imposed at the upstream domain pressure-inlet and the temperature set to a value higher than OAT. Constant velocities and temperature at the free turbine exit representing an engine at MTOP rating were used at the computational domain inlet. Turbulence intensity was considered to be 4% and the viscosity ratio set to 10.

The higher the pressure losses caused by the engine compartment, the smaller the entrained airflow and thus the pumping ratio. The curve of pumping ratio vs. engine compartment pressure drop is known as the ejector characteristic curve and can be considered to be a straight line. This way, for each configuration, two computations with different imposed total pressures at the pressure-inlet suffice to characterize the ejector. The operating pumping ratio can then be obtained once the engine compartment losses are estimated.

The performance of the exhaust system was evaluated by two main parameters:

- Pumping ratio:

(1) $$\phi = \frac{\dot{m}_{secondary}}{\dot{m}_{primary}}$$

- Recovery pressure:

(2) $$C_p = \frac{\overline{p}_{s\ \ ejector} - \overline{p}_{s\ \ inlet}}{\hat{p}_{dyn\ \ inlet}}$$

where $\overline{p}_{s\ \ ejector}$ and $\overline{p}_{s\ \ inlet}$ is the area-weighted average of the static pressure at the indicated plane and $\hat{p}_{dyn\ \ inlet}$ is the mass-weighted average of the dynamic pressure at the inlet plane.

Note that the pressure losses are related to C_p as $\Delta P = f(M^2)(1-C_p)$. On the hypothesis that C_p is independent of Mach number[8], maximizing the pressure recovery corresponds to minimizing the pressure losses.

In 2D analysis, a third output parameter was also considered: the slope of the ejector characteristic curve which represents the robustness of the ejector, i.e. if the pumping ratio is more or less sensitive to engine compartment pressure drop changes. In reality, other parameters such as the system mass must as well be taken into account in the exhaust system design.

3.2. Parameterization and design exploration

A classic Central Composite Design (CCD) method was employed to generate a Design of Experiments (DOE) screening set. It allows determining the overall behavior of the meta-model to be fit. For N parameters, a CCD design consists of one central point, $2N$ points located at $\pm\alpha$ positions on the axis of each input parameter and $2^{(N-f)}$ points located at ± 1 on the diagonals of the input parameters space, where f is the fraction of the

factorial design and α is a distance to the input parameter space center defined to minimize the variance inflation factor (VIF-optimality). In this way, the 2D analysis initial DOE comprised 45 design points while the 3D DOE comprised 79.

For the response surface creation, a Kriging method was used. This algorithm combines a global approximation of the design space with localized deviations in order to pass a function through all the sample points. The interpolation function $y(x)$ can be written as:

$$y(x) = f(x) + Z(x) \quad (3)$$

where $f(x)$ is a polynomial function of the parameters set and $Z(x)$ is a normal distribution with mean zero. With the auto-refinement option, new design points are created and the response surface is updated until the maximum relative error is below a user-defined value.

The model was created and parameterized using Ansys DesignModeler®. The list of all input parameters is presented in Table 1.

Table 1 Examples of geometric and aerodynamic parameters considered in this study

	Parameter
Primary nozzle	Exit diameter Length Concavity (shape)
Ejector	Lip radius Straight part length Diffuser length Diffuser opening Concavity (shape) Elbow angle (3D only)
Relative position	Axial distance (standoff) Radial distance (gap) Decentering (3D only)
Aerodynamic	Inlet swirl (3D only)

4. RESULTS

4.1. Axisymmetric 2D analysis

This preliminary axisymmetric 2D study was performed to provide a first comprehension of the flow inside the ejector and to identify a few parameters whose influence on the performance is small. This is important because the quality of the response surface is strongly dependent on the number of input parameters.

Initially, a total of 10 geometric parameters was studied: primary nozzle length, concavity and exit diameter (3), ejector lip radius, straight part and diffuser part lengths (3), diffuser opening and concavity (2) and axial and radial distances between primary nozzle and ejector (2). The swirl was not investigated in this particular case and the ejector presented no elbow, since the objective was an axisymmetric 2D computation.

4.1.1. Parameters reduction

In order to try to reduce the number of input parameters, the correlation between different input parameters and the sensitivities of output to input parameters were evaluated. Spearman correlation between two variables is a measure of their monotonous dependence and is defined as:

$$r = \frac{\sigma_{xy}}{\sigma_x \sigma_y} \quad (4)$$

$$\sigma_{xy} = \sum_i (rank(x_i) - \bar{x})(rank(y_i) - \bar{y}) \quad (5)$$

$$\sigma_x = \sqrt{\sum_i (rank(x_i) - \bar{x})^2} \quad (6)$$

300 samples were generated with Latin Hypercube Sampling method which generates points whose correlation between the input parameters are below 5% and uniformly distributed.

Figure 3 shows the parameters correlation to the output parameters. First of all, one can see that the correlations of the ejector length and the ejector diffuser length have the same values, meaning that they affect in a similar way the solution. Therefore, only one of these two parameters is necessary and the other one can be fixed (ejector length).

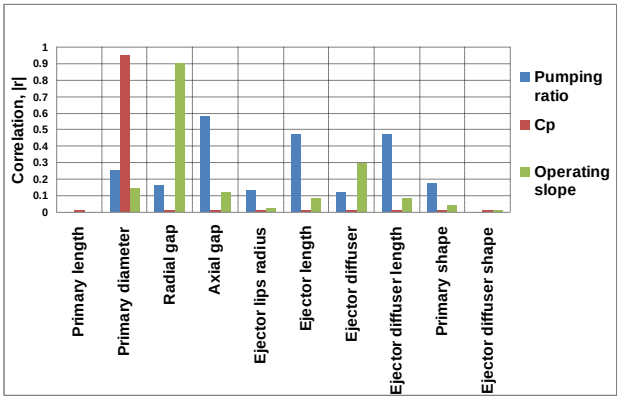

Figure 3 Input/output parameters correlation

Secondly, it is seen that two parameters have almost zero correlation to the output: primary nozzle length and ejector diffuser shape. This information alone is not sufficient to conclude that those parameters have little impact on the performances. In this case, an analysis of the sensitivities of the solution to the parameters is necessary. For example, regarding the ejector diffuser opening and shape, one can observe in Figure 4 that although the variation of the pumping ratio with the diffuser opening is important, its shape does not significantly modifies the profile of the curves. Further investigations of several configurations and a similar study of the primary nozzle length show this same behavior of the solution, allowing the elimination of these parameters (ejector diffuser shape and primary length) as design ones.

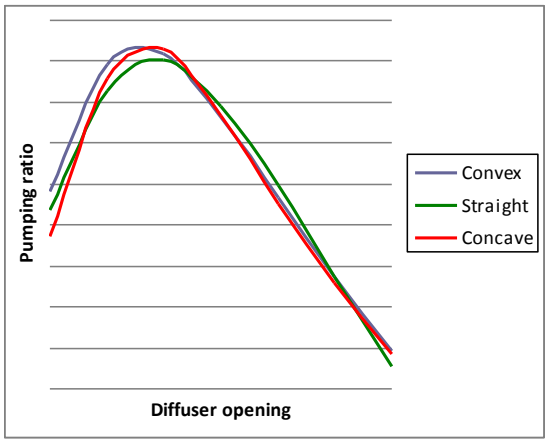

Figure 4 Pumping ratio as a function of the ejector diffuser opening and shape.

Finally, two parameters have small correlation (<0.2): ejector lip radius and primary nozzle shape. Their sensitivities show that as far as the ejector lip radius is concerned, beyond a given value (red line in Figure 5), the changes in the output parameters are smaller than 1% and for this reason it will not be kept for the response surface generation. The primary nozzle shape however does affect the pumping ratio, as shown in Figure 6 and must thus be kept as a design parameter.

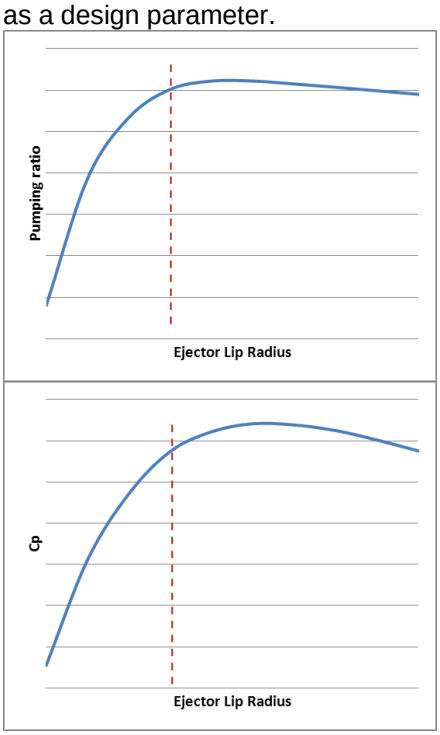

Figure 5 Pumping ratio and Cp as a function of the ejector lip radius. Beyond the red line the variation of these quantities represents less than 1%

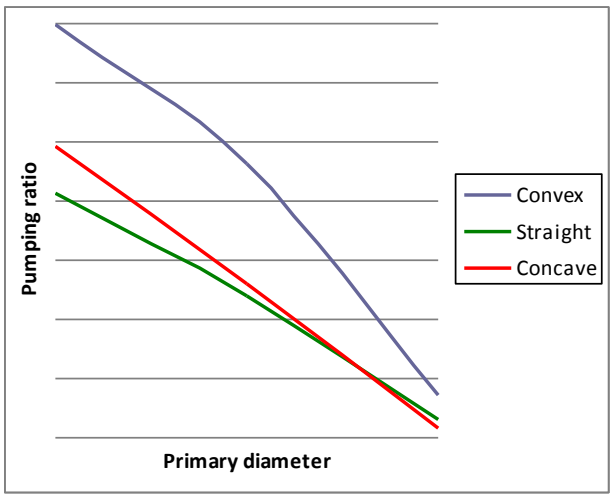

Figure 6 Pumping ratio as a function of the primary diameter and shape.

Though not represented here, C_p and operating slope follow the same trends as the pumping ratio, i.e. their sensitivities to the eliminated design parameters are also negligible. In this way, the number of design parameters could be reduced from 10 to 6.

4.1.2. Response surface analysis

45 design points were used to generate the response surfaces and 3 refinement points were automatically added to the DOE by the Kriging

method to achieve a maximum relative error of 8% in the response surface approximation.
After the parameters reduction study, two primary nozzle parameters were kept for further analysis: the exit diameter (divergence) and the shape (concave, conical or convex). Figure 7 represents response surface approximations of the pumping ratio and C_p as a function of the primary nozzle divergence and its shape.

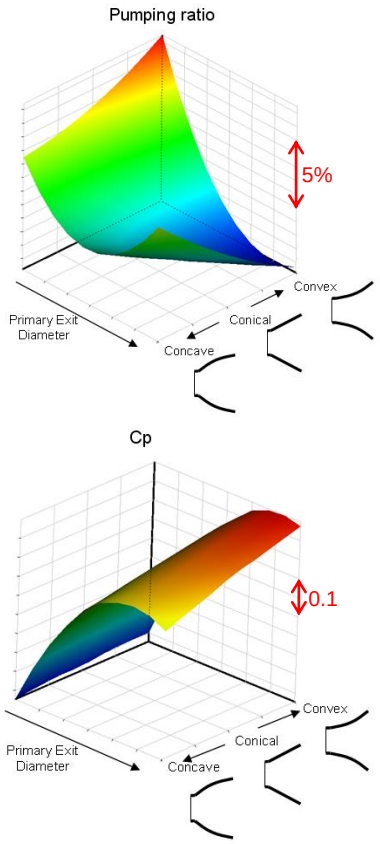

Figure 7 Response surface approximations of the pumping ratio and C_p as a function of the primary nozzle exit diameter and shape.

They highlight the opposing evolution of the two output parameters with the nozzle exit diameter: C_p increases as the nozzle becomes more divergent whereas the pumping ratio is favored by a convergent nozzle. Indeed, the smaller the nozzle exit area the higher the velocities at this surface and the smaller the static pressure, which helps the entrainment of the secondary airflow through the gap. The cost in power loss though can be very important (reduction by a factor of three between red and blue regions on the response surface), that is the reason why engine manufacturers prefer to equip the engines with a divergent nozzle. Regarding the primary nozzle shape, one can notice that on one side its impact on pressure recovery (and thus on power losses) is quite small but on the other side a concave (also known as bell shaped) divergent nozzle could improve the pumping ratio. In this case, this quantity increases by 15%.

Concerning the ejector, response surfaces presented in Figure 8 show that a long ejector is preferred for maximizing the pumping ratio and also increasing the pressure recovery. This conclusion is valid for ejectors in the length range considered, namely for L/D_E between 1.5 and 3.6. For the diffuser opening, one can see that both response surfaces reach a maximum. Indeed, increasing the ejector exit area decelerates the flow and causes the static pressure to increase. However, beyond a certain diffusion, the flow separates from the walls and the pressure drop becomes more important. Optimum area ratio varies from 1.32 for short ejectors to 1.7 longer ones (within the studied range).

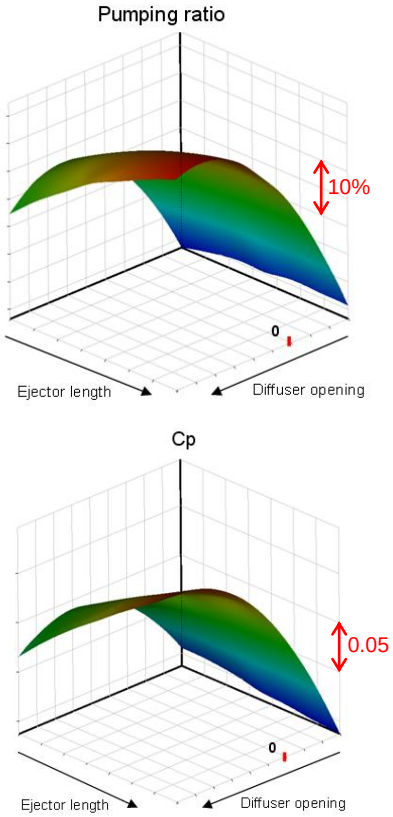

Figure 8 Response surface approximations of the pumping ratio and C_p as a function of the ejector length and the diffuser opening.

Finally, the influence of the relative position (axial and radial) between primary nozzle and ejector on the pumping ratio is analyzed in Figure 9, which presents the pumping ratio response surface approximation as a function of these two parameters. The maximum is found to be at $D_E/D_N = 1.7$ and with maximum negative standoff

computed, namely $s/D_N = -0.27$. However, due to important engine movements during flight, an exhaust system with such an axial distance is not acceptable for safety matters as the risk of directing the engine hot gases directly into the compartment is high. For this reason, the standoff is usually set to zero.

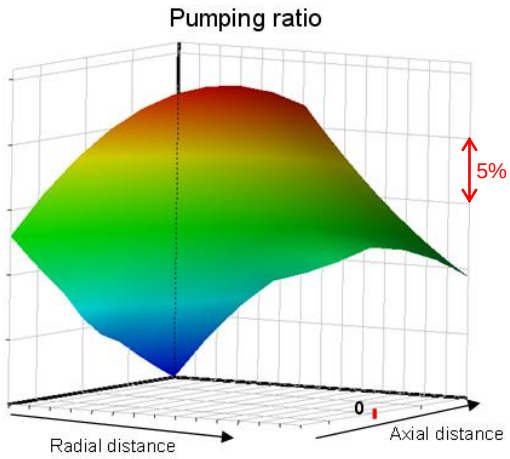

Figure 9 Response surface approximation of the pumping ratio as a function of ejector and primary nozzle relative position (radial and axial distances)

In addition, the radial distance between primary nozzle and ejector comes out as an important parameter for the robustness of the ejector. Indeed, the operating slope quickly decreases when the gap becomes important (Figure 10).

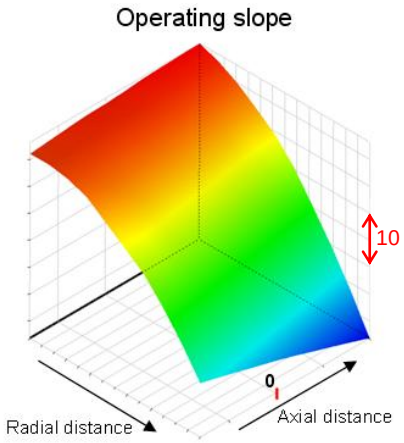

Figure 10 Operating slope response surface as a function of ejector and primary nozzle relative position (radial and axial distances)

4.2. 3D analysis

To the 2D reduced list of parameters, 3 additional ones were included for the 3D analysis: nozzle/ejector axes decentering, ejector elbow angle and inlet flow swirl.

It is supposed that the influence of the parameters pointed out in the 2D analysis as having a small impact on the performance is still negligible in the 3D study and so they are set to a fixed value hereafter. A later verification of this hypothesis should be performed.

4.2.1. Ejector elbow angle and swirl

The effect of the inlet swirl on the flow is illustrated in Figure 11, which shows a comparison between contours of axial velocity within an ejector with no elbow for two cases: without swirl and with 30° swirl.

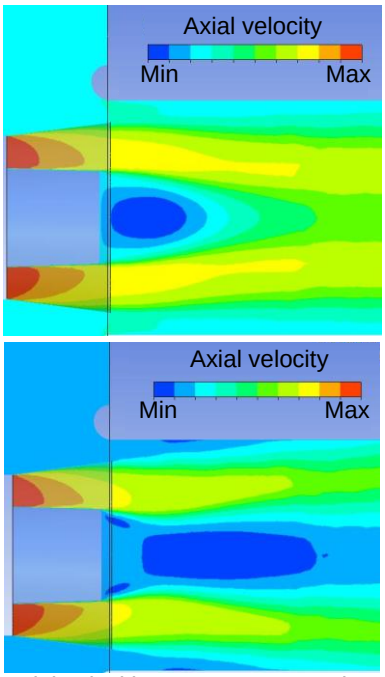

Figure 11 Axial velocities contour at z=0 plane. Detail of primary nozzle and ejector inlet. Comparison between a non-swirling flow (top) and a 30°-swirl (bottom) inlet flow.

One can notice that the swirl centrifuges the jet towards the ejector wall creating a small separation bubble and a blockage for the secondary flow. Indeed, the separation zone downstream the central body is almost 2 times longer and the velocities at the gap decrease by 65% from one case to another.

The presence of an elbow at the ejector breaks the rotational symmetry and severely modifies the flow. A double blockage effect is observed: the outer part of the elbow stands as a wall and forces the flow to deviate towards the inner part, which causes an increase in the pressure up to the ejector entrance and thus to reduce the pumping ratio. Figure 12 represents the pressure contour of a non-swirling flow within a 40°-elbowed ejector at the elbow plane, highlighting the high adverse pressure the secondary flow faces at the ejector inlet.

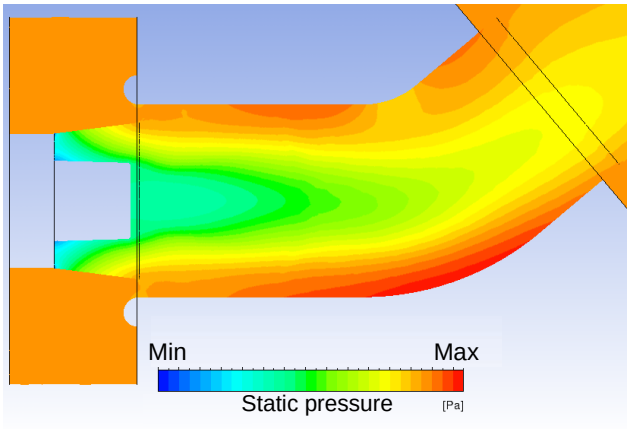

Figure 12 Pressure contour within a 40°-elbowed ejector. The inlet swirl swirl is set to 0°

In Figure 13 one can see that though elbow angle and inlet swirl individually usually have a negative impact on the exhaust system performances they are strongly coupled and could, depending on the conditions, combine in a way to attenuate this effect. Indeed, for a given elbow angle, there is an inlet swirl which maximizes the pumping ratio. While the maximum value decreases with the elbow angle, the optimal swirl increases with it. This comes from the fact that an important elbow angle causes a strong blockage and the swirl may favor the flow in other directions filling the separation downstream of the inner part of the elbow. However, beyond the optimum, the losses due to swirl become more significant and the pumping ratio tends to decrease.

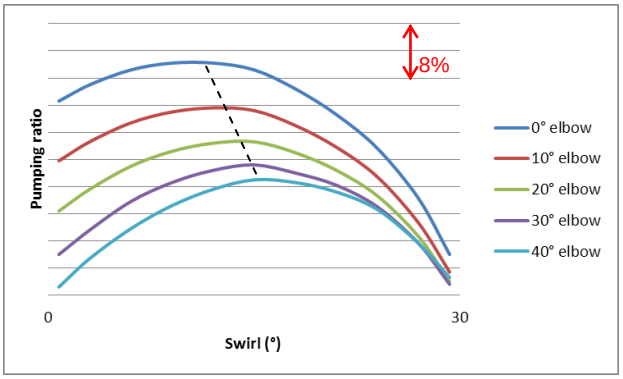

Figure 13 Pumping ratio as a function of the flow swirl for different ejector elbow angles: Optimum in swirl varies with the elbow angle

Unfortunately, these two parameters can rarely be considered as design ones, since the swirl is function of the engine rating and thus varies during the flight and the exhaust direction is primarily chosen to avoid reingestion.

4.2.2. Gap between nozzle and ejector

The ejector diameter being weakly correlated to other parameters, its impact on the performance is analyzed separately, for a given primary nozzle diameter. Figure 14 shows the evolution of pumping ratio and C_p as a function of the gap size for a 40° elbowed ejector and no inlet swirl. One can observe that both performance parameters increase with the gap size, but the pumping ratio reaches a maximum at $D_E/D_N = 1.6$. Beyond this value, the Venturi effect of the gap becomes less effective and the presence of the ejector downstream of the primary nozzle is less and less perceived by the nozzle (C_p continues to increase).

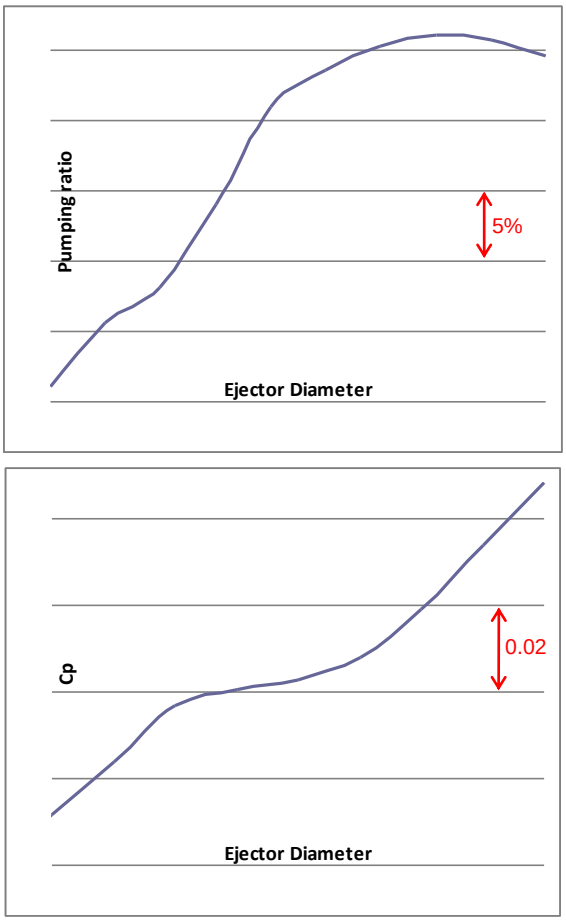

Figure 14 2D slices of pumping ratio and C_p response surface approximations as a function of the ejector diameter

When primary nozzle diameter varies as well as the gap size, the curves of pumping ratio as a function of the gap size evolve as shown in Figure 15. For example, compared to the baseline design, a reduction of 4% in the primary nozzle diameter conserving the same pumping ratio allows reducing the ejector diameter by 9%, a non negligible gain in mass.

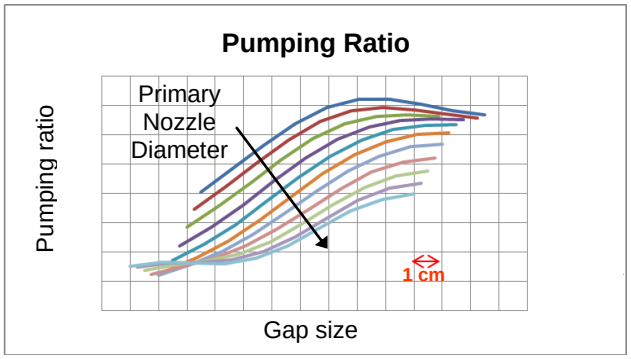

Figure 15 Pumping ratio as a function of the radial distance between ejector and primary nozzle (gap) for different primary nozzle exit diameters (increase direction indicated by the arrow)

4.2.3. Decentering

Engine decentering is simulated by a radial displacement of the nozzle in relation to the ejector and in this study it consists only in a decentering in the elbow plane. It is defined as positive when towards the inner elbow and negative otherwise. The maximum value (positive and negative) of the displacement corresponds to 7% of the gap size. Figure 16 represent 2D slices of pumping ratio and C_p response surfaces as a function of engine decentering. The ejector angle is set to 40° and there is no swirl in the inlet flow.

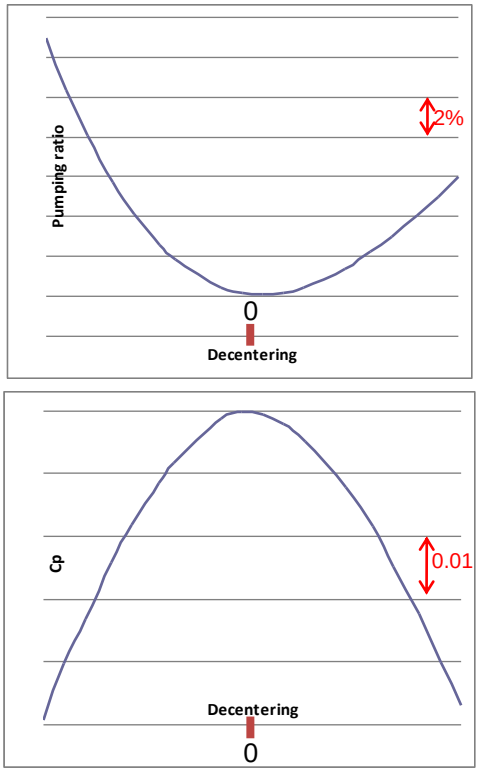

Figure 16 2D slices of pumping ratio and C_p response surface approximations as a function of the decentering for a 40° elbowed ejector and no inlet swirl

Positive or negative, the decentering always causes the losses to increase (since Cp decreases), but it favors the pumping ratio. However, the changes in the performance parameters are not symmetrical: for a given displacement, the pumping ratio in further increased when the nozzle is towards the outer part of the elbow. Comparing the velocity magnitude contours of both cases one notices that they are quite similar (Figure 17). As previously discussed, the elbow degrades the performances due to the blockage it creates, but by negatively decentering the nozzle, the velocities at the gap are increased on the lower part, smoothing the flow at the elbow.

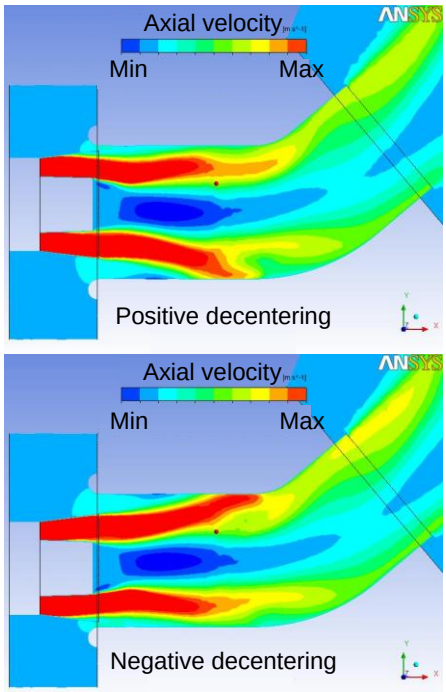

Figure 17 Axial velocities contour at z=0 plane. Detail of primary nozzle and ejector inlet. Comparison between positive (top) and negative (bottom) decentering.

The decentering appears as a fine-tuning parameter (in reality it is limited by the gap size and manufacturing/installation tolerances) allowing to slightly increase the pumping ratio with small penalty in terms of losses.

5. CONCLUSION

In this study, fully-automated axisymmetric 2D and 3D CFD computations of a parameterized model were carried out in order to investigate the influence of the main aerodynamic design parameters on the performance of a helicopter exhaust system.

2D analysis allowed eliminating some design parameters having little impact on the performance of the ejector. It was also possible to highlight the conflicting behavior of the output parameters to changes in the geometry. Most importantly, it was

shown that a bell shaped primary nozzle could help improving the pumping ratio by 15% with negligible impact on the pressure recovery (compared to a straight one with same exit area). Although a negative standoff seems to provide better results in terms of pumping ratio, safety constraints usually prevent such designs on a helicopter. Finally, it was found that the radial gap between ejector and primary nozzle (or the area ratio) is a major parameter for the robustness of the ejector.

In the 3D CFD analysis, a strong coupling between ejector elbow and inlet swirl was observed. In addition, it was pointed out that, despite a small negative effect on the pressure recovery, decentering the ejector and primary nozzle axes makes the pumping ratio increase and could therefore be used as a fine tuning design parameter.

Further studies on this topic should take into consideration that the research of an optimum design of a helicopter exhaust system must be defined by a multi-objective optimization process and more globally it must also be included in a multi-disciplinary optimization process, integrating mechanical, thermal and manufacturing constraints.

6. REFERENCES

[1] F. Toulmay, “Internal Aerodynamics of Infrared Suppressors for Helicopter Engines”, AHS 40th Annual Forum, 1984
[2] B.D. Vyas and S. Kar, "Study of Entrainment and Mixing Process for an Air to Air Ejector", 1975
[3] C.C. Folkman, « An Advanced Method For Predicting The Performance Of Helicopter Propulsion System Ejectors », AHS 48th Annual Forum, 1992
[4] A.L. London and P.F. Pucci, “Exhaust Stack Ejectors For Marine Gas Turbine Installations”, USA Stanford University Dept. Mech. Eng. TR26, 1955
[5] G. Sovran and E.D. Klomp, « Experimentally Determined Optimum Geometries for Rectilinear Diffusers with Rectangular, Conical or Annular Cross-Section”, Fluid Mechanics of Internal Flow, 1st Edition, Elsevier, pp270-319, 1967
[6] M.G. Anderson, “FLUENT CFD versus Sovran & Klomp Diffuser Data Benchmark Study”, 46th AIAA Aerospace Sciences Meeting and Exhibit, AIAA 2008-665, 2008
[7] S.F. McBean, A.M. Birk, “CFD (Realizable $k-\varepsilon$) and Cold-flow Testing for the Design of Ai-air Ejectors with Triangular Tabbed Driving Nozzles”, ASME Turbo Expo 2007, Power for Land, Sea and Air, GT2007-27632, 2007
[8] J. Gräsel, J. Demolis, H. Mohr and H.-P. Schiffer, « Multi-Objective Design Optimisation of A Diffuser-Ejector Exhaust Duct for Helicopter Engines », ASME Turbo Expo 2010, GT2010-22588, 2010